Al-Azhar University Civil Engineering Research Magazine (CERM)
Vol. (41) No. (1) January, 2019

Assessment the Global Precipitation Measurement Mission (GPM) Rainfall Product over Sinai

Mahgoub, M. [(1)] Amin, D*.[(1)] Hemdan,T*. [(2)] Basiony, M. [(2)]
(1) Water Resources Research Institute, WRRI, NWRC Egypt.
(2) Civil Engineering Department, Benha Faculty of Engineering - Benha University.

ملخص
يعتبر عدد المحطات الأرضية لرصد الأمطار في سيناء قليل جداً ، مما يجعلها غير قادرة على تمثيل توزيع الأمطار على سيناء خاصة في المناطق الجبلية. تهدف هذه الدراسة إلي تقييم بعثة قياس هطول الأمطار العالمية (GPM)لتقدير هطول الأمطار فوق سيناء. تم إستخدام سلسلة زمنية للبيانات الشهرية خلال الفترة (2000-2016) لعدد عشرة محطات أرضية لقياس المطر للمقارنة مع منتج الأمطار GPM خلال نفس الفترة ، وقد تم إستخدام المعايير الإحصائية للتأكد من دقة المنتج GPM لهطول الأمطار حيث تم إستخدام متوسط خطأ الجذر (RMSE)، معدل الإنحراف المعياري (RSR) ، Nash Sutcliffe (NSC) ومعامل الإرتباط (r) , وقد تم تصحيح بيانات القمر الصناعي GPM بإستخدام معامل الإنحراف الشهري (BFs) عن طريق المقارنة مع المحطات الأرضية لرصد الأمطار. وأظهرت النتائج بعد التصحيح أن إنحراف هطول الأمطار في GPM ليس له إتجاه ثابت حيث يتم المبالغة في تقدير الأمطار في بعض المحطات والتقليل منها في البعض الآخر. يعمل معامل الإنحراف (BF) على تصحيح بيانات GPM وقد أظهرت النتائج تحسينًا في أداء بيانات GPM كما أظهرت أيضاً أن المعايير الإحصائية مقبولة.

ABSTRACT
The rainfall stations in Sinai are very scarce, that make them not be able to represent the rainfall distribution over Sinai especially in mountainous regions. This paper aims to evaluate the Global Precipitation Measurement Mission (GPM) in estimating rainfall over Sinai. The monthly data time series during the period (2000-2016) for ten rain gauge stations were used to compare with the GPM rainfall product during the same period. In order to assess the GPM rainfall product accuracy, the statistical criteria; Root mean square error (RMSE)-observations Standard Deviation Ratio (RSR), Nash Sutcliffe (NSC) and correlation coefficient (r) were used. The GPM data is bias corrected using the monthly Bias Factors (BFs) reference to the observed rainfall gauge data. The results show that GPM rainfall bias has no fixed direction where it is overestimated in some stations and underestimated in others. The BF correct the GPM data and the results show enhancement in the performance of the GPM data and accepted statistical criteria.

Keywords: Rainfall estimation, Satellite images, (GPM), Statistical Criteria.

1. Introduction
Precipitation is one of the most essential parameters in the earth system, where it is used in many hydrological applications. Therefore, it is important to accurately understanding and monitoring precipitation patterns. There are two infield methods to measure precipitation; gauge and weather radars. Gauges provide the most accurate precipitation observations. However, gauge data are provided at specific sites with spare rain gauges network. The weather radar can provide the time series of real-time with high resolution monitoring over large areas. However, its network is not dense enough over all parts of the world (Tang, Ma, Long, Zhong, & Hong, 2016). The rainfall

estimation using satellite images applications can be a good source of data. The GPM mission is launched on 2014, provides a spatial resolution of 0.1° × 0.1°grid (Krishna, Das, Deshpande, Doiphode, & Pandithurai, 2017). Many studies are concerned with assessing the performance of satellite images rainfall products and most conclusions indicated that the accuracy of satellite precipitation products such as Tropical Rainfall Measuring Mission (TRMM) decreases in mountainous regions (Duan, Liu, Tuo, Chiogna, & Disse, 2016), to overcome this issue the GPM core satellite carries a Dual-frequency Precipitation Radar (DPR) that consists of a Ka-band precipitation radar (KaPR) operating at 35.5 GHz that measures light rain and a Ku-band precipitation radar (KuPR) operating at 13.6 GHz which measures moderate-to-heavy rain(Gaona, Overeem, LeijNSC, & Uijlenhoet, 2016). So it's the first satellite that can detect light and solid precipitation more accurately than any other product. (Prakash et al., 2018) provides a comprehensive assessment of two GPM high resolution products namely, Integrated Multi-satellite Retrievals for GPM (IMERG) and Global Satellite Mapping of Precipitation (GSMaP), The two GPM products are compared with Tropical Rainfall Measuring Mission (TRMM) and gauge-based observations over India, the results show that the precipitation values from the GPM products are significantly improved. The rain gauge data are used to evaluate the GPM product for four different topography and climate conditions in Iran for only one year, the results show that GPM is more accurate than other rainfall products in all study regions (Sharifi, et al., 2016). (Tang et al., 2016) In 2016 used 2200 observed rain gauge data, across Mainland China, to evaluate the quality of TRMM and GPM. He found that GPM show better performance compared with TRMM at 3-hourly and daily resolutions. The GPM product compared with the CPC Morphing technique (CMORPH) over the Blue Nile basin it found that GPM skills in detecting rainfall events is better than CMORPH (Sahlu, Nikolopoulos, Moges, Anagnostou, & Hailu, 2016). (Wang, Chen, & Wang, 2017) compare GPM and TRMM satellite products with ground precipitation data in the coastal region of china for a two-year period from 2014 to 2015, the statistical metrics show that both satellite products underestimate the observed rainfall values but GPM products provide a slightly better performance than TRMM. (Murali Krishna, Das, Deshpande, Doiphode, & Pandithurai, 2017) and (Gabella, Speirs, Hamann, Germann, & Berne, 2017) also found that the GPM product performs well and suitable to be used in hydro-climatic applications but the satellite rainfall estimation over mountainous regions remains a challenge.

2. Study Area

Sinai Peninsula is located in the far northeast of Egypt between Gulf of Aqaba and Gulf of Suez and situated between the Mediterranean Sea from north and the Red Sea from south serving as a land bridge between Asia and Africa (Afandi, Morsy, & Hussieny, 2013). Sinai geographic co-ordinates are 29° 29' 59.99" N and 33° 49' 59.99" E (Gaber, Koch, & El-Baz, 2010), it has a population of approximately 1,400,000 capita. . In addition, Egyptians also refer to it as the land of turquoise. Sinai represents about 6% of Egypt's area which is about 61,000 km^2 (Abd El-Ghani, Huerta-Martínez, Hongyan, & Qureshi, 2017).

Sinai has a triangular shape, its southern topography consists of rugged, sharply mountains which reach to elevations more than 2000 meters as shown in fig (1) (El Kenawy, et al., 2010). The mountains distinguish the southern topography of Sinai, Gebel Musa (2,285 m), and Gebel Serbal (2,070 m) and Egypt's highest mountain is Mount Catherine, its height reaches to (2,641m), Mount Catherine receives approximately 50 mm/year of precipitation, partly as snow (Gaber et al., 2010). The

central area consists of two plateaus, Al-Tih and Al-Ajmah, both deeply indented and dipping towards the north. Along the Mediterranean Sea, the northward plateau slope is broken by shaped hills that reach to 100 meters height and there are parallel lines of sand between the hills and the coast (Effat & Hassan, 2013).

Sinai is an Arid to Semi-arid region, which characterized by hot weather. Its high temperature increases near the north coast and over mountains. Precipitation values decreases from the northeast towards the southwest, the greatest amount of the annual rainfall was found at Rafah station (304 mm) in the northeast and the annual rainfall average is about 120mm along the Mediterranean coast. In the southern region, the annual rainfall is reached to 20 mm in the coastal areas over the Gulfs of Aqaba and Suez and increases to 70 millimetres over the mountain regions (Afandi et al., 2013).

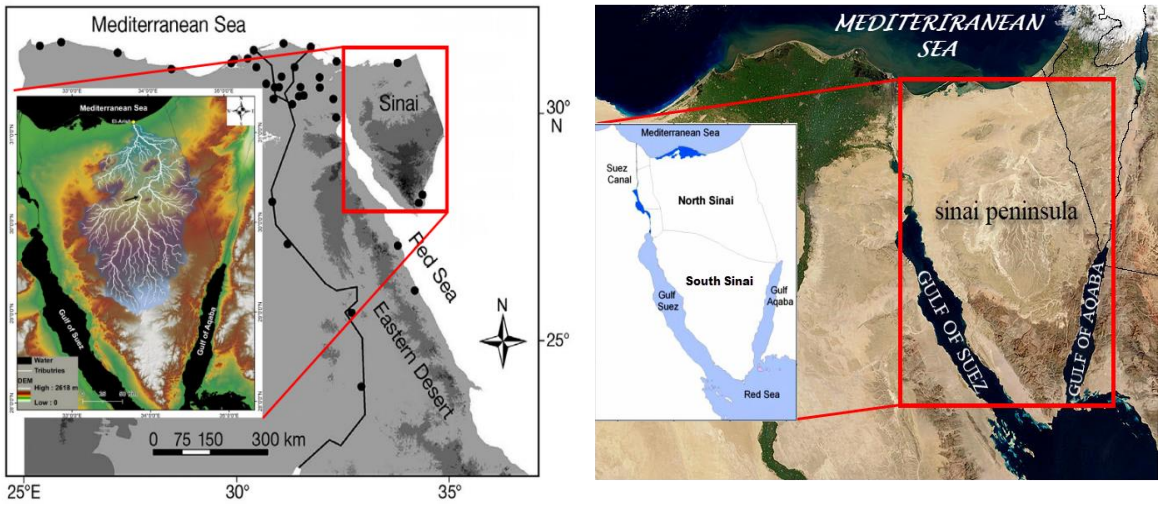

Figure (1): Sinai Peninsula (The study area).

3. Data Sets and Methodology:

A monthly time series data for 10 rain gauge stations were used to evaluate the GPM data for the same period. Section 3.1 and 3.2 describe the observed rain gauge data and the GPM data respectively. Four statistical criteria were used in the comparison; RSR Moriasi et al. (2007), NSC, correlation coefficient and BIAS. The BF was used to correct the bias between the observed and the GPM product. The projections on the corrected data on the daily extreme events were analyzed.

3.1 Surface Rain Gauge Data:

The data set used in the study includes the rainfall data obtained from the Egyptian Meteorological Authority (EMA). EMA has about nineteen stations distributed throughout North and South Sinai as shown in fig (2). Based on the availability of the ground observed data, some stations were excluded due to the gaps in the data time series.

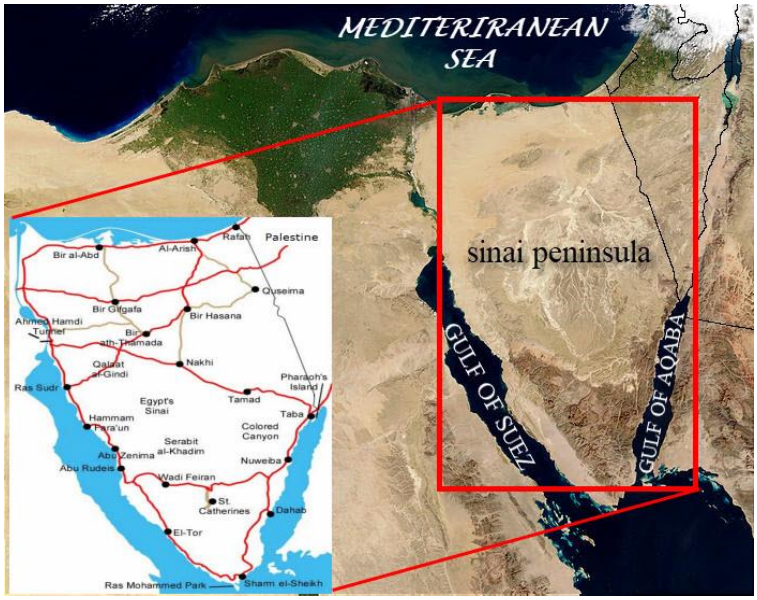

Figure (2): Distribution of EMA Rainfall Stations in Sinai.

3.2 GPM Rainfall Data:

GPM is an international satellite mission to provide next-generation observations of rain and snow worldwide every three hours. GPM provides hourly temporal resolution rainfall data with a great coverage of 60°N-60°S as shown in fig (3) (Huffman, 2017). the 24 hours average (daily data mm/hr) temporal resolution are used to Obtain the monthly values for the selected ground monitoring stations in order to correct the data and disaggregate the corrected data to daily data again. GPM product has two versions, Version5 product covers the period from March 2000 to November 2010 and theVersion6 product starts from March 2014 to present, and it is available at http://sharaku.eorc.jaxa.jp/GSMaP/ at hourly and daily time scales.

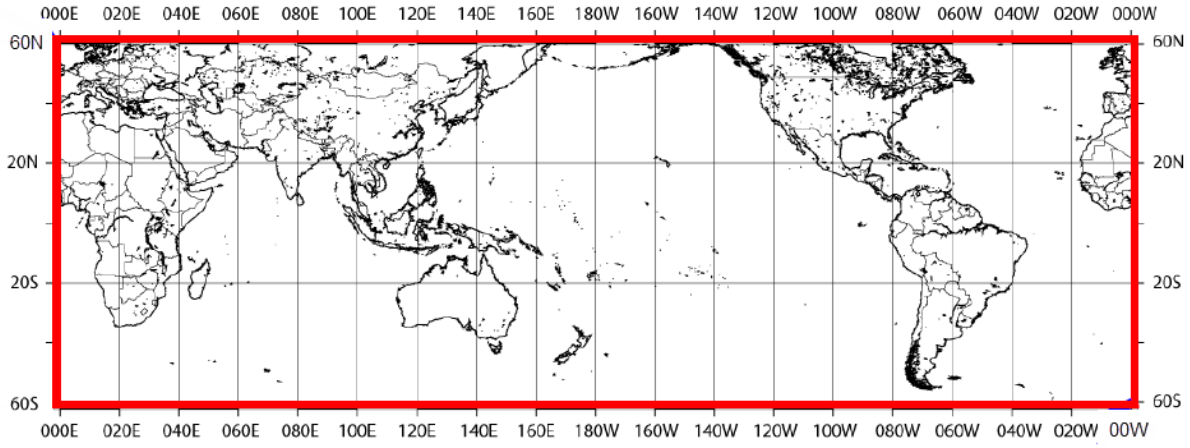

Figure (3): The GPM Data Coverage Map.

.

3.3 The Methodology:

The GPM rainfall product is calibrated using the observed rain gauge data. Statistical criteria such as RSR, NSC, and correlation coefficient (r) are used to assess the accuracy of the GPM, where:

$$\boldsymbol{RSR} = \frac{\boldsymbol{RMSE}}{\boldsymbol{STDFV_{obs}}} = \frac{\sqrt{\sum_{i=1}^{n}(Z_s - Z_o)^2}}{\sqrt{\sum_{i=1}^{n}(Z_o - \bar{Z}_o)^2}} \quad (1)$$

$$\boldsymbol{NSC} = \mathbf{1} - \left[\frac{\sum_{i=1}^{n}(Z_o - Z_s)^2}{\sum_{i=1}^{n}(Z_o - \bar{Z}_o)^2}\right] \quad (2)$$

$$\boldsymbol{r} = \left[\frac{n\sum(Z_o Z_s) - (\sum Z_o)(\sum Z_s)}{\sqrt{(n\sum(Z_s)^2 - \sum(Z_s)^2)\,(n\sum(Z_o)^2 - \sum(Z_o)^2)}}\right] \quad (3)$$

***Where**: Zs the rainfall gridded data product, Zo the observed rainfall from the rain-gauge station and $\bar{Z}o$ is the mean of the observed rainfall.*

The RSR is a normalized error index that utilizes the benefits of the RMSE that is one of the frequently used error index statistics (Onema et al., 2012). GPM product can be judged as satisfactory if RSR < 0.70, while zero is the optimum value (Moriasi et al., 2007). The NSC is used to compare the performance of the GPM relative to the observed rain gauges. NSC can take values between –∞ and 1. A value of 1 indicates a perfect agreement between GPM product and observed rain gauge data and a value of zero indicates that the GPM product does not explain any part of the initial (observed) variance. A negative value indicates that the GPM product is worse than the observed data. The correlation coefficient (r) is used to assess the agreement between the GPM satellite data and the rain gauge observations, r ranges between -1 and +1; the r value close to +1 indicates a perfect positive fit while negative values indicates a weak linear correlation (Wang & Lu, 2016).

The monthly BFs were calculated between the mean monthly of GPM data and the Observed mean monthly for the ten locations of the rain gauges. The calculated bias factors were used to correct the Monthly GPM data product and projected that correction on the daily extreme events to be used effectively for the hydro-climatic applications, where:

$$\boldsymbol{BIAS} = \frac{\sum_{i=1}^{n}(Z_s)}{\sum_{i=1}^{n}(Z_o)} \quad (4)$$

The GPM rainfall values were corrected using the calculated bias factors to be in order to get corrected daily time series that can be used in the hydrological applications, (Saber & Yilmaz, 2016).

Where:

$$\boldsymbol{GSMAPcorr} = \frac{\boldsymbol{GSMAP}}{\boldsymbol{Bias\ Factor}} \quad (5)$$

GSMaPcorr: The corrected GSMaP data,

GSMaP: GSMaP data before corrections from the satellite maps.

4. Results and Discussions :

4.1 Evaluation of the GPM Monthly Data

The comparison between the monthly GPM time series was performed with reference to the observed monthly rain gauge data for 17 yrs. The stations divided into three parts; the first part includes stations located in the north area which involve Rafah and Arish

stations, the second part includes Nekhel, Meliz and Hasana stations which are located in the middle of Sinai and the last part includes the stations located in the south of Sinai. The statistical criteria were applied and show that the GPM precipitation values overestimated the observed gauge data in the total monthly scale for all studied stations, figures 4, 5 ,6 indicate scatter plot for the total monthly precipitation comparison between satellite and gauge data. The correlation coefficient (r) shows acceptable results in most stations. The RSR and NSC criteria show unsatisfactory results. After the bias correction procedure, the GPM rainfall Bias has no fixed trend, it is overestimated the gauges values in some stations and underestimated in others, the performance of the GPM were improved. However the rainfall pattern become closer to the observed pattern, see table (1).

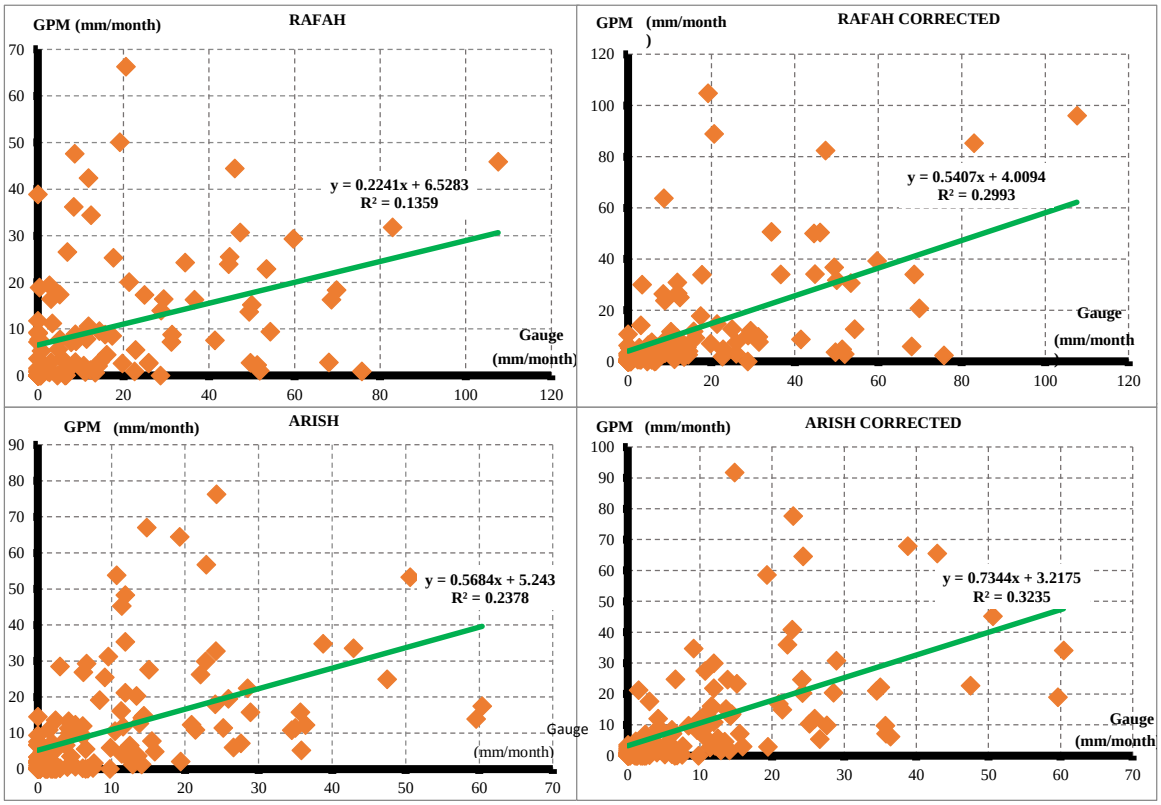

Figure (4): scatter plot for the total monthly precipitation comparison between satellite and gauge data for North Sinai stations.

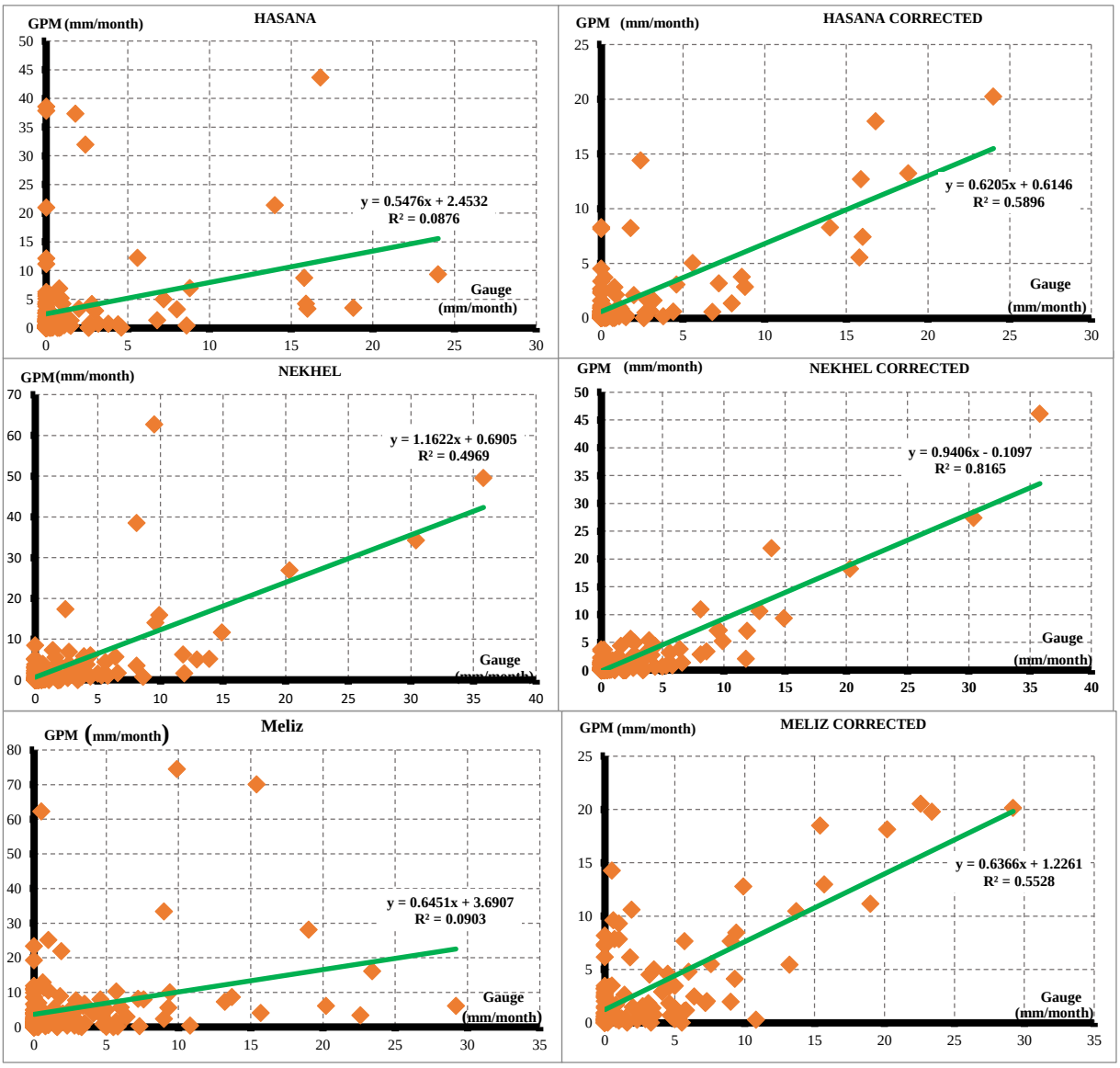

Figure (5): scatter plot for the total monthly precipitation comparison between satellite and gauge data for Middle Sinai stations.

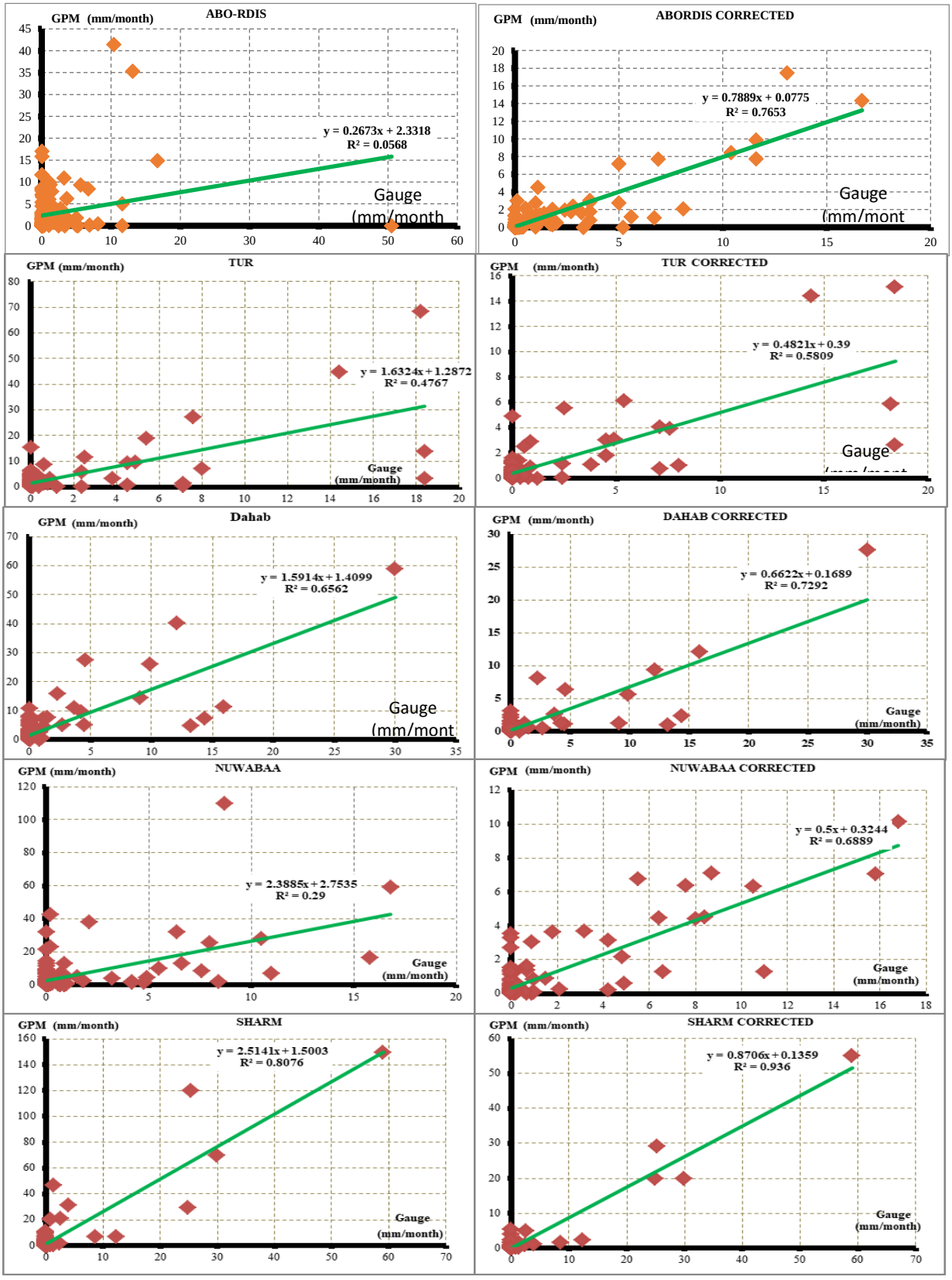

Figure (6): scatter plot for the total monthly precipitation comparison between satellite and gauge data for South Sinai stations.

Table (1): Statistical Metrics Resulting from Comparison before and after Bias Correction.

No.	Stations	r		RSR		NSC	
		Before	After	Before	After	Before	After
1	Rafah	0.37	0.55	0.81	0.77	0.13	0.29
2	Arish	0.49	0.57	1.1	1.09	0.24	0.32
3	Hasana	0.52	0.77	2.42	0.64	0.09	0.59
4	Meliz	0.51	0.74	1.91	0.68	0.09	0.55
5	Nekhel	0.82	0.9	0.95	0.45	0.49	0.82
6	Dahab	0.82	0.85	1.79	0.53	0.66	0.73
7	Tur	0.55	0.76	3.67	0.67	0.48	0.58
8	Nuwabaa	0.67	0.83	4.28	0.61	0.29	0.69
9	Rdis	0.61	0.87	3.85	0.49	0.06	0.77
10	Sharm	0.89	0.97	1.82	0.26	0.81	0.94

The plot visualization graphs for the mean monthly GPM compared with the mean monthly-observed data show generally overestimation for all station locations in Sinai, see Figure (7), (8) and (9).

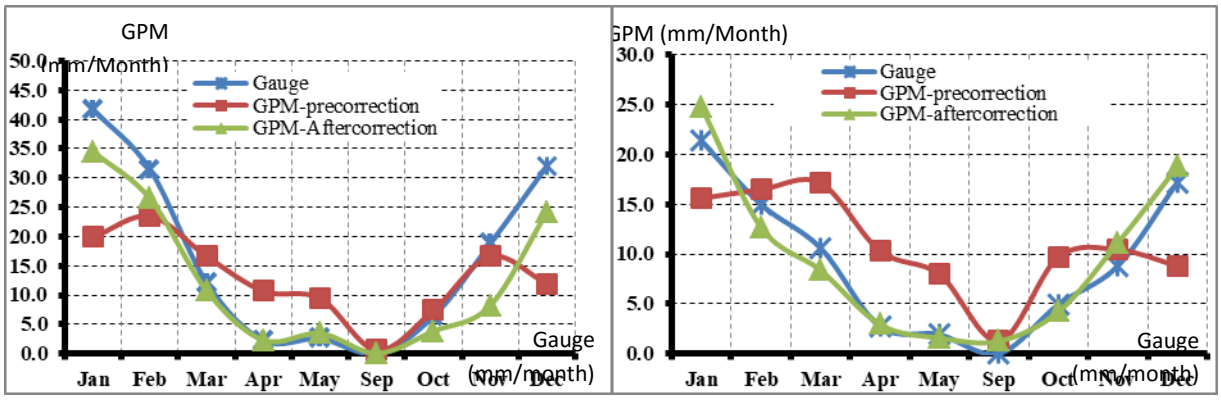

Rafah Station Arish Station

Figure (7): Total monthly average precipitation comparison in North Sinai.

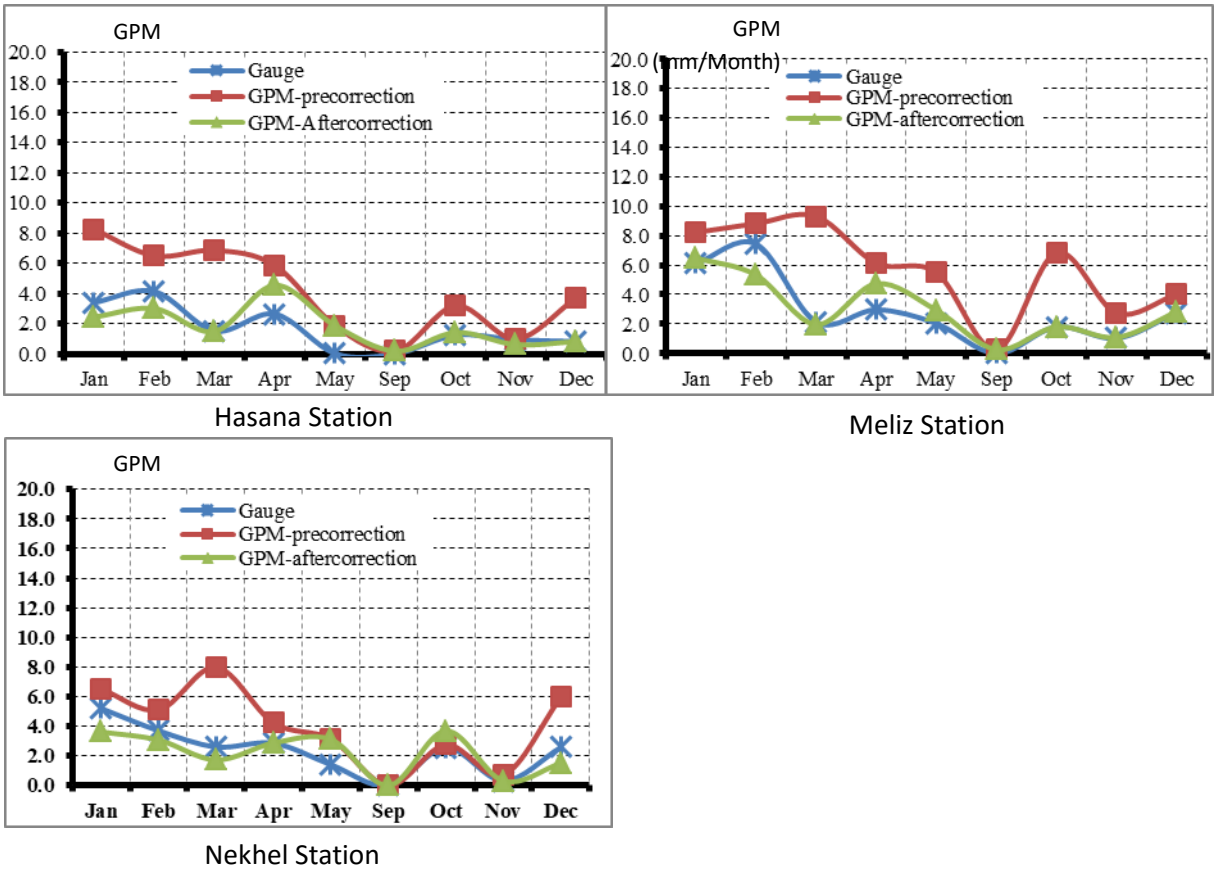

Figure (8): Total monthly average precipitation comparison in Middle Sinai.

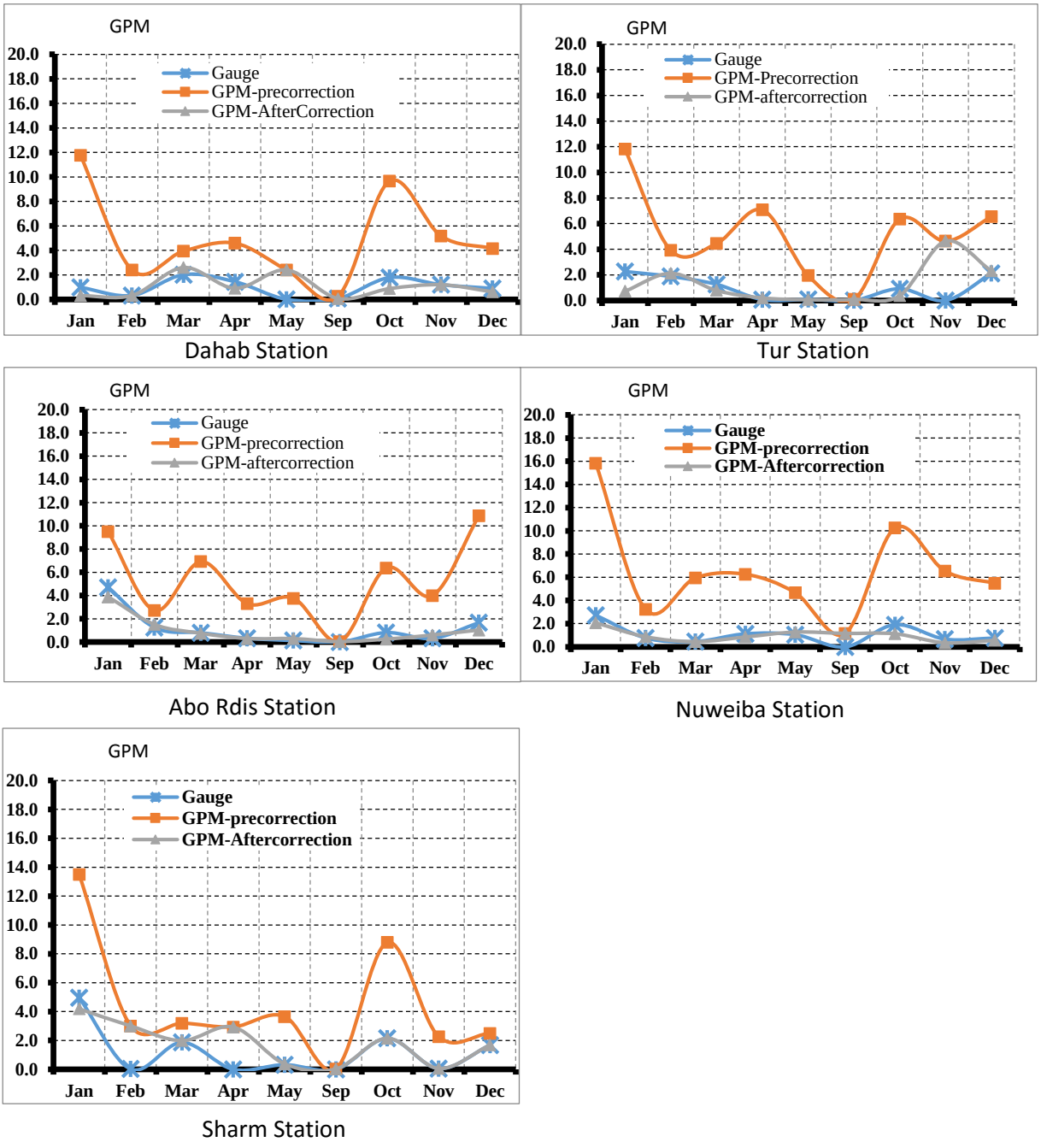

Figure (9): Total monthly average precipitation comparison in South Sinai.

4.2 Projection of the Bias Correction on the Extreme Events:

Based on the availability of flood events observed by the referenced rain gauges of EMA stations; 16 flood events from the year 2000 to 2017 were studied. Using the correction coefficient showed a better improvement in statistical analysis, it shows a strong correlation coefficient between satellite and observed data in most stations, the RMSE and MAE are relatively small and the RSR and NSC statistical metrics show acceptable results as shown in table (2).

Table (2): Statistical Metrics Resulting from Projection of the Bias Correction on the Extreme Events.

NO.	STATIONS	r		RMSE		MAE		RSR		NSC	
		Before	After	Before	After	Before	After	Before	After	Before	After
1	ABO-RDIS	0.709	0.838	4.084	3.865	3.160	2.532	0.847	0.801	0.283	0.358
2	ARISH	0.854	0.948	2.935	2.777	2.570	2.370	0.668	0.632	0.553	0.600
3	DAHAB	0.997	0.995	5.955	3.810	3.583	3.230	0.468	0.299	0.781	0.910
4	MELIZ	0.729	0.854	3.885	3.276	2.843	2.079	0.787	0.664	0.380	0.559
5	TUR	0.914	0.983	2.486	1.686	1.949	1.404	0.434	0.294	0.812	0.914
6	HASANA	0.721	0.786	4.006	3.921	2.810	2.121	0.807	0.790	0.348	0.375
7	NEKHEL	0.866	0.956	4.628	2.755	2.515	1.916	0.657	0.391	0.568	0.847
8	NUWABAA	0.932	0.933	5.868	4.787	3.483	3.114	1.105	0.902	-0.222	0.187
9	RAFAH	0.860	0.872	4.273	3.835	3.078	3.199	0.564	0.506	0.682	0.744
10	SHARM	0.994	0.992	3.714	2.941	2.088	1.888	0.350	0.277	0.878	0.923

5. Conclusions:

The main conclusions of this study are to assess the capability of using the Global Precipitation Measurement (GPM) rainfall satellite imagery product in rainfall estimation to overcome the difficulties of using the ground rainfall stations. GPM within the time period from 2000 to 2016 was calibrated using ground rain gauge network in Sinai. Ten stations were selected from EMA network based on the availability of precipitation data. Statistical analysis such as correlation coefficient, Bias, NSC and RSR were performed to evaluate the accuracy of satellite data. The results of the analysis indicated that the GPM satellite data are reasonably correlated with rain gauge data with a varying overestimation bias. Bias factors were computed to multiplicatively correct the GPM data using rain gauge observations. After applying the bias factor; the statistical criteria were reasonably improved, it showed accepted values and the GPM rainfall Bias has no fixed trend. The calculated bias corrections were applied on the available extreme events during the time period from 2000 to 2017 to assess the accuracy of GPM rainfall data on extreme events, The statistical criteria shows a good linear correlation between the measured and observed data, RSR and NSC shows

accepted values. The research recommends using GPM satellite rainfall data in different hydrological applications after calculating bias factors to correct the satellite data bias.

REFERENCES*:*

- Abd El-Ghani, M. M., Huerta-Martínez, F. M., Hongyan, L., & Qureshi, R. (2017). Plant respoNSCs to hyperarid desert environments. *Plant RespoNSCs to Hyperarid Desert Environments*, 1–598.
- Afandi, G. El, Morsy, M., & Hussieny, F. El. (2013). Heavy Rainfall Simulation over Sinai Peninsula Using the Weather Research and Forecasting Model, *2013*.
- Duan, Z., Liu, J., Tuo, Y., Chiogna, G., & Disse, M. (2016). Evaluation of eight high spatial resolution gridded precipitation products in Adige Basin (Italy) at multiple temporal and spatial scales. *Science of the Total Environment*, *573*, 1536–1553.
- Gabella, M., Speirs, P., Hamann, U., Germann, U., & Berne, A. (2017). Measurement of precipitation in the alps using dual-polarization C-Band ground-based radars, the GPMSpaceborne Ku-Band Radar, and rain gauges. *Remote Sensing*, *9*(11).
- Gaber, A., Koch, M., & El-Baz, F. (2010). Textural and compositional characterization of Wadi Feiran deposits, Sinai Peninsula, Egypt, using Radarsat-1, PALSAR, SRTM and ETM+ data. *Remote Sensing*, *2*(1), 52–75.
- Gaona, M. F. R., Overeem, A., LeijNSC, H., & Uijlenhoet, R. (2016). First-Year Evaluation of GPM Rainfall over the Netherlands: IMERG Day 1 Final Run (V03D). *Journal of Hydrometeorology*, *17*(11), 2799–2814.
- Huffman, G. J. (2017). Status and Results from the Day-1 Integrated Multi-Satellite Retrievals for GPM (IMERG), (1), 2017.
- Krishna, U. V. M., Das, S. K., Deshpande, S. M., Doiphode, S. L., & Pandithurai, G. (2017). Earth and Space Science, 540–553.
- Murali Krishna, U. V., Das, S. K., Deshpande, S. M., Doiphode, S. L., & Pandithurai, G. (2017). The assessment of Global Precipitation Measurement estimates over the Indian subcontinent. *Earth and Space Science*, *4*(8), 540–553.
- Prakash, S., Mitra, A. K., AghaKouchak, A., Liu, Z., Norouzi, H., & Pai, D. S. (2018). A preliminary assessment of GPM-based multi-satellite precipitation estimates over a monsoon dominated region. *Journal of Hydrology*, *556*(February 2014), 865–876.
- Sahlu, D., Nikolopoulos, E. I., Moges, S. A., Anagnostou, E. N., & Hailu, D. (2016). First Evaluation of the Day-1 IMERG over the Upper Blue Nile Basin. *Journal of Hydrometeorology*, *17*(11), 2875–2882.
- Tang, G., Ma, Y., Long, D., Zhong, L., & Hong, Y. (2016). Evaluation of GPM Day-1 IMERG and TMPA Version-7 legacy products over Mainland China at multiple spatiotemporal scales. *Journal of Hydrology*, *533*(December), 152–167.
- Wang, R., Chen, J., & Wang, X. (2017). Comparison of IMERG level-3 and TMPA 3B42V7 in estimating typhoon-related heavy rain. *Water (Switzerland)*, *9*(4), 1–15.